jas

LEAKAGE FLOW-INDUCED VIBRATION OF AN UNCONSTRICTED TUBE-IN-TUBE SLIP JOINT*

by

T. M. Mulcahy

Materials and Components Technology Division
ARGONNE NATIONAL LABORATORY
Argonne, Illinois 60439

December 1986

DISCLAIMER

Paper to be presented at the ASME Vibration Conference, Boston, Massachusetts, September 27-30, 1986.

*Work supported by the U. S. Department of Energy, Office of Basic Energy Sciences, under Contract W-31-109-Eng-38.

LEAKAGE FLOW-INDUCED VIBRATION OF AN UNCONSTRICTED TUBE-IN-TUBE SLIP JOINT

by

T. M. Mulcahy
Materials and Components Technology Division
Argonne National Laboratory
Argonne, IL 60439

ABSTRACT

The conditions are given for which the more flexible of two cantilevered, telescoping tubes conveying fluid can be self-excited by flow leaking from an unconstricted slip joint. Also, a physical explanation of the excitation mechanism is discussed, and a design rule to avoid the mechanism is presented. In addition, the results for the unconstricted slip joint are shown to be similar to those for slip joints having annulus constrictions at very short engagement lengths.

I. INTRODUCTION

Main coolant flow paths through the components of energy conversion and utilization systems often parallel each other from one relatively constant-pressure plenum to another. However, the flow paths and plenums are rarely completely sealed from each other because designs must allow for removal and thermal expansion of components. Thus, leakage flow across pressure boundaries is not uncommon. When component vibration can interact and alter the leakage flow, the conditions for self-excited vibrations are present. Many energy system component designs have suffered from leakage flow-induced vibrations (examples of reactor component vibration are given in Refs. 1-3).

Recently an experimental study was concluded [4-7] that identified the conditions for leakage flow excitation associated with a specific tube-in-tube slip joint formed where the free ends of two cantilevered tubes conveying fluid overlap (telescope together), a common structural configuration in energy conversion systems. A short, raised diameter on one of the tubes produced an annulus constriction in the slip joint flow geometry, which was a known source of self-excitation. Although design rules were formulated [7],

self-excitation without an annulus constriction was observed for the first time during testing. This was unexpected, based on the available physical explanation of the self-excitation mechanism [2,8-10]. However, self-excitation has been reported for slip joints without annulus constrictions [11]. Thus, a need for further study was indicated. Here, the existing physical explanation of the excitation mechanism is interpreted to include unconstricted slip joints, and the new experimental results are presented.

II. SELF-EXCITATION MECHANISMS

Center Bodies

A physical explanation of the self-excitation mechanism for axisymmetric center bodies almost completely blocking the flow in a channel with an annulus constriction has been developed [8] and verified by experiment and theory [9]. Consider Fig. 1, where the flow in a rigid, stationary tube is obstructed by a long center body shaped to create a very short, narrow annulus constriction at its left end. Assume the pressure difference between A and B is constant and the flow is from left to right. This upstream annulus constriction can be shown to create conditions for self-excitation.

To appreciate the mechanism, give the rigid center body a uniform velocity upward. Then the pressure gradient in the upper and lower channels of the annulus must be similar to those shown to decelerate the fluid in the (upper) channel above the center body, where the annulus constriction is instantaneously closing, and to accelerate the fluid in the (lower) channel below the center body, where the annulus constriction is instantaneously opening. The resultant flow force on the center body due to the pressure distribution is in phase with the velocity of the body, and therefore represents a destabilizing source of self-excitation. If the center body is flexibly mounted, the flow force can be interpreted as negative damping that will produce self-excited vibrations when it is larger than the positive structural damping. If the flow is from right to left in Fig. 1, a center body with a downstream annulus constriction is formed. Using rationalizations similar to those just given, stabilizing forces and positive flow damping can be shown to exist for a vibrating center body [8]. These rules-of-thumb

are strictly valid only for long center bodies with short, terminal constrictions. An expanded, more fundamental explanation of the excitation mechanism is required if more general cases are to be included.

Slip Joints

Figure 2(a) shows a configuration more common in industrial practice: a simple slip joint formed at the free ends of two telescoping tubes. For the flow direction shown, the slip joint has a center body (tube) with an upstream annulus constriction. If the center tube were flexibly supported and the outside rigid-fixed, the conditions of Fig. 1 would prevail and negative, destabilizing damping would be predicted, at least for $L \ll LD$. However, the upper (center) tube is identified as rigid and fixed, while the lower (outer) tube is identified as flexible in lateral translation to represent the fundamental cantilevered mode motion recently tested [7]. These conditions are the reverse of the structural support conditions of Fig. 1. Also, L is not necessarily small compared with LD.

The pressure variations on the outside tube will be similar to those on the center body of Fig. 1, but their effect on the excitation of the outside tube will require interpretation. First, the net flow force on the outside tube will be different from that on the inside tube, since the exposed flow surfaces of the outside tube extend upstream as well as downstream from the annulus constriction. Second, for L on the order of LD, the parallel flow in the narrower gap of the annulus constriction cannot be ignored. In essence, the outside tube is subject to the effects of: a destabilizing upstream annulus constriction, as discussed for the center body of Fig. 1; parallel flow in the constriction, which, if relatively long and narrow, can produce significant positive flow damping [12]; and a downstream restriction to flow passing along the wall of the flexible tube upstream of the slip joint, which is stabilizing, as explained next. The pressure variations exerted on the flexible tube by the flow entering into the modulating slip joint is believed to be a significant source of positive flow damping for the limiting case of a short or nonexistent annulus downstream from a short constriction.

The presence and stabilizing effect of the slip joint as a downstream restriction to flow along the wall of the flexible tube is best visualized by letting LD = 0.0 and L be very small, in which case the large annulus between

the tubes is eliminated; see Fig. 2(b). The raised diameter no longer functions as a constriction to a larger downstream annulus, but merely forms an **unconstricted slip joint** with a narrow gap. In any case, when the slip joint opening is modulated, the outside tube is exposed only to wall pressure variations upstream of the unconstricted slip joint. For flow from A to C in Fig. 2(b), the restriction of the slip joint is downstream, but there is no annulus. The analogous situation is created in Fig. 1, with flow from right to left, by eliminating the channel walls to the right of the constrition. In both cases, even without the annulus, the flow along the flexible wall must decelerate (accelerate) when the unconstricted slip joint instantaneously closes (opens). Thus, the pressure at C in Fig. 2(b) must instantaneously increase (decrease), while the ambient pressure at A remains the same, to produce a pressure gradient that instantaneously retards (promotes) the rate of flow through the unconstricted slip joint. The instantaneous increase (decrease) of pressure distribution along the tube wall opposes the instantaneous closing (opening) of the unconstricted slip joint, and therefore can be interpreted as a stabilizing flow force or positive damping. This limiting geometry for producing positive flow damping was not recognized at the time of testing, but positive damping was measured for short L and the data will be presented later.

As for a center body, stabilizing forces are produced on the outer tube in Fig. 2(c) by the flow in the annulus upstream of the annulus constriction, and by the parallel flow in the narrow annulus of the constriction. In fact, at the time of testing, these sources were expected to provide positive flow damping for all conditions. This thinking was reinforced by earlier testing with large L, $L/W' \geq 25$, which showed no self-excitation for any $LD \geq 0$. However, when testing was performed with $L/W' \leq 13$, self-excitation occurred for the configuration of 2(c) at $LD < 0.4$ R. Similar self-excitation was observed for two other design variations as long as $IL < 0.4$ R, including $IL < L$. The details of this experimental evidence will be presented after the physical explanation is broadened to include these new observations.

Again the contribution of pressure forces on the outside tube created by the flow accelerating or decelerating along the wall downstream from the restriction, where no annulus existed, were not appreciated. The flow from C to A in Fig. 2(c), modulated by vibration of the slip joint, still produces

negative damping and the potential for self-excitation when LD and L are small. The reasoning is the same as given for the center body of Fig. 1, but with the walls of the channel eliminated downstream from the constriction. In effect, the basic excitation mechanism exists without the walls, but the confining effect of the walls acts as an amplifier by forcing all the flow modulation and pressure recovery closer to the flexible surface. Thus, larger downstream annuli will have a weaker excitation potential; a small L/W' is required because self-excitation cannot occur unless the positive damping produced by parallel flow through the constriction is less than the negative damping produced over A to C.

When LD is very small or zero (Fig. 2(c)), the upstream annulus effect is eliminated and the annulus constriction becomes essentially an unconstricted slip joint. Thus, the two telescoping tubes shown in Fig. 3(b), which have no raised diameter, can be expected to produce flow conditions from C to A similar to those in Fig. 2(c). Also, self-excitation of an unconstricted slip joint can be expected for short engagement lengths. This was observed and will be discussed.

With the insight described above, an even broader physical explanation can be formulated for the self-excitation of any flexible surface that forms a restriction to leakage flow driven by a constant pressure differential, including slip joints with or without annulus constrictions. In essence, fluid forces that promote negative damping and, hence, self-excitation, are created on that part of the flexible surface exposed to the accelerating and decelerating flow **emanating from** a modulating restriction. That is, flexible surfaces subject to modulating pressure recovery forces have the potential to be self-excited. Fluid forces that impair self-excitation by contributing to positive damping are created on that part of the flexible surface exposed to accelerating and decelerating flow **converging into,** or flow already in, a modulating restriction. Also, confining more of the modulating flow closer to the flexible surface will amplify fluid damping and self-excitation potential. Self-excitation occurs when the distribution of negative damping dominates the positive damping, including structural damping. Not surprisingly, one form or another of this generalized physical explanation has been used to explain the self-excitation of piping valves, hydraulic flow control gates, nuclear fuel blades, etc. [1,2].

III. TESTS

Three slip joint configurations were tested at the free ends of the same two cantilevered tubes. The slip joints having a sharp edge and beveled annulus constriction are shown in Figs. 2(a) and 3(a), respectively, while the unconstricted slip joint is shown in Fig. 3(b). The constriction radius R was ~ 5 in. (127 mm). Flow damping and critical velocities for self-excitation were determined for the much more flexible of the two cantilevered tubes, which was ~ 16 ft (4.9 m) long and had a fundamental natural frequency of ~ 3.1 Hz. The much shorter, relatively rigid tube had a fundamental frequency of ~ 85 Hz.

Not only could the slip joint configurations be interchanged, but different end pieces for the same configuration were available to change the length L and gap W' of the constrictions. Also, for each test piece, the engagement length IL and fundamental mode damping of the flexible tube could be varied independently. Further, the position of the shorter tube could be moved to achieve initially concentric or any eccentric alignment of the free tube ends, including initially contacting tubes. All tests reported here are for initially concentric alignment, which could be maintained within ± 6% of the radial gap W'.

The flowrate through the slip joint was measured by several turbine flow meters, and the average velocity in the constriction V was determined by dividing the flowrate by the constriction's flow area. Flow velocities were measured in the range of 0.5–50 ft/s (0.15–15.2 m/s) with an accuracy of ± 4%. The flow direction through the slip joint could be reversed with valves in the flow facility. The static pressure drop across the slip joint was measured using two differential pressure transducers covering the range of 0.1–50 lb/in.^{2} (670 Pa–345 kPa). The pressure transducers were very linear (± 2%) but zero drift problems with the strain gage bridges limited accuracy at low pressure readings to ± 0.025 lb/in.^{2} (± 172 Pa). The motion of the flexible tube was measured at the slip joint using two displacement gauges, orthogonal to each other, that functioned in the range of ± 0.050 in. (± 7.75 mm). The proximity (eddy current) gauges were not linear over their range, so they were set up such that deviations around zero displacements were no more than ± 0.0005 in. (± 0.013 mm) while deviations at the extremes of the range could be as large as ± 0.003 in. (± 0.08 mm).

In general, critical flow velocities were identified as those for which structural plus flow damping, or total damping, became zero. The total damping in the first mode ζ_1 was determined by averaging the percent of critical damping obtained from the decaying displacement transients of three pluck tests. Each pluck test was initiated at a different amplitude in the range 0.0025 in. (0.064 mm) to 0.006 in. (0.015 mm) to give the most repeatable results. At larger initial amplitudes, the transient motion could have been influenced by nonlinear effects produced by the constriction's annular gap W', which was as small as 0.020 in. (0.51 mm) in some tests. Initial first mode damping in the range from ζ_0 = 0.1 to 8% of critical was measured before and after flow testing, while the presence of flow could increase the total damping ζ_1 to 25% or reduce it to zero. For no flow, the damping measurements were repeatable within ± 10%.

The repeatability of the damping measurements with flow was variable, depending more on the physical phenomena than on the ability to accurately measure amplitudes and time from transient decay curves. Because of the presence of turbulence in the flow, the measurement of total damping became increasingly inaccurate as the velocity increased, to the point where damping could not be measured. However, in 75% of the cases of self-excitation, the damping decreased rapidly with flowrate. Thus measurement accuracy was similar to that for no flow. For the remaining cases of self-excitation that occurred at high flow velocities, the change in spatial motion of the slip joint, from a random orbit to a highly directional and pseudoperiodic motion, also was used to identify critical flowrates. This procedure was highly subjective and inaccuracies in these critical velocities up to ± 25% may be present. In the case where damping increased with flow, the largest damping reported was repeatable within ± 25%.

Further details of the test facility, test procedures, and instrumentation are available [5].

IV. DISCUSSION OF TEST RESULTS

Self-Excitation of Unconstricted Slip Joints

Critical reduced flow velocities $V/2f_1R$ for the slip joint with no annulus constriction and the flow direction of Fig. 3(b) are given in Fig. 4 as a function of engagement length and gap size. Table 1 shows that the tests were performed for a wide range of parameters, but self-excitation of the flexible tube was observed only for very short engagement lengths, IL < 1.0 in. (25.4 mm), and only when the flow was in the direction shown in Fig. 3(b)--the conditions for instability identified in Section II. Thus an annulus constriction is not necessary for self-excitation at short engagement lengths, only flow emanating from the slip joint and impinging on the flexible tube surface. However, this self-excitation source is weak relative to the annulus constriction mechanism. Parallel flow in a slip joint with greater than 20% of a diameter of engagement evidently produced enough positive damping to dominate the self-excitation mechanism. Maintaining engagements greater than 20% of the diameter is a simple and easily implemented design rule-of-thumb to avoid self-excitation of unconstricted slip joints.

Table 1. Geometry with No Annulus Constriction

R = 2.74 in. (139.2 mm)	W' = 0.040 in. (1.02 mm)
IL = 0.125 to 4.0 in. (3.18 to 101.6 mm)	= 0.141 in. (3.58 mm)
ζ_o = 0.5, 3.3% of the critical damping	= 0.282 in. (7.16 mm)

The relative weakness of the excitation mechanism became clear when the extent of the excitation mechanism was explored. Clearly the critical velocities in Fig. 4 depend on the engagement length and the annular gap. Generally, up to engagement lengths of 20% of R, lower critical velocities occurred for smaller IL and W', negative damping was measurable (Figs. 5-8), and deterministic limit-cycle motion was observed beyond the critical velocities. However, as the engagement length was increased in the range $20\% < IL/R \leq 40\%$, the flow damping quickly became positive while the self-excitation weakened and disappeared.

There was concern that a forced excitation was being observed instead of self-excitation, because the variation in the critical reduced velocities of Fig. 4 were relatively small over the range of small IL and W'. Also, forced excitation due to vortices shed in annuli [3] had been identified as an excitation mechanism for similar geometries. Therefore several tests were performed for W'/R = 1.4% at significantly larger initial damping, $\zeta_o \sim 3\%$. Critical velocities were found to be increased significantly, as shown by the solid symbols in Fig. 4. Also, the flow damping data for $\zeta_o \sim 3\%$ at IL/R = 4.6% and 9.1% formed reasonable extensions of the data obtained at the smaller $\zeta_o \sim 0.5\%$, as shown by the solid symbols in Figs. 5 and 6. This supports the self-excitation hypothesis and the choice of $\zeta_1 - \zeta_o$ as the damping measure.

The damping data for an unconstricted slip joint at large ζ_o and IL/W' = 18.3% did not match well with the small ζ_o data below $V/2f_1R = 1.5$. No definite reason can be given for the discrepancy, but air trapped upstream of the slip joint was observed in other cases to produce spurious results until swept away at higher flows.

Unconstricted Slip Joints in Reverse Flow

No self-excitation was observed for the unconstricted slip joint when the flow direction was opposite that of Fig. 3(b). In terms of the mechanisms proposed in Section II, neither an annulus constriction nor flow emanating from the slip joint and impinging on the flexible tube exist to create the conditions necessary for self-excitation. In fact, the conditions that exist were hypothesized in Section II to be stabilizing. As argued for the case of Fig. 2(b), the converging flow trying to escape through the modulating slip joint will create positive damping forces from A to C even as the engagement length IL approaches zero. This trend was exhibited by the test data.

Flow damping measurements are shown in Fig. 9 for three gap sizes, W'/R = 1.4, 5.1, and 10.3%, and engagements in the range $1.83 \geq IL/R \geq 0.05$. The engagement of 0.125 in. (3.18 mm) was the smallest practical for a tube radius of R = 2.74 in. (69.6 mm). Always, the damping was found to be positive with a definite dependence on gap size W', as can be seen by comparing curves in 9(a)-(c) at the same IL/R. A more significant trend is the decrease in damping that occurs with a decrease in engagement length over

the large range tested. Apparently the damping converges to a finite, positive value for IL = 0, based on a comparison of the damping for the three smallest IL, which are half the next largest IL. That is, since parallel flow in the slip joint was eliminated, only the flow from A to C can be the source of positive damping at IL ~ 0, as suggested in Section II. Note that the minimum damping curves for each W' in Fig. 9 are nearly the same.

Unconstricted Slip Joint Pressure Differential

The pressure differential was observed to be the same for both flow directions through the slip joint when W'/R = 1.4%. When W'/R = 5.1% and 10.3%, the pressure differential for the flow direction shown in Fig. 3(b) was always lower than the differential for the reversed flow direction, but the differences were never greater than ~ 25%. Also, variations in the pressure differential with changes in engagement length IL and gap size W' were much smaller than variations in the flow damping.

Data obtained for IL/R = 4.6, 36.5, and 182.5% are shown in Figs. 10(a) and (b). Measurements were made for four other engagements, but, for clarity, only the extremes and one intermediate engagement length are shown. There are small measurable differences in the trend lines (least squares fit) for the three different values of IL for W'/R = 1.4%, shown in Fig. 10(a), but none were measurable for W'/R = 5.1 and 10.3%, as shown in Fig. 10(b). The data not shown for other intermediate engagement lengths fall between or on the data shown in Fig. 10. In fact, the data in Fig. 10(b) for different W' essentially define the same trend line, and this trend line is very similar to that in Fig. 10(a) for the shortest engagement length. Evidently the pressure losses due to flow friction in the annulus of the slip joint are small compared with the entrance and exit losses of the slip joint.

The general insensitivity of the pressure differential to variations in engagement length and gap size implies that the velocity parameter in Figs. 4-9 could be replaced by a ΔP parameter, and the trends in the data would change very little. Also, the insensitivity means that ΔP is not responsible for the large increases in damping that occur with increases in engagement length. This observation supports the supposition of Section II that parallel flow in the annulus, which does depend on channel length and gap size [10], is responsible for the increases in flow damping.

Self-Excitation of Sharp-Edge Annulus Constrictions

Also shown in Figs. 5 and 6 are the damping data associated with the self-excitation of the sharp-edge annulus constriction of Fig. 2(c) with W'/R = 1.4%, W = 0.282 in. (7.16 mm), two short engagement lengths IL/R = 9.1% and 18.3% at LD = 0.0, and two initial damping levels of $\zeta_o \sim 0.5\%$ (open symbols) and 3.3% (solid symbols). In addition, damping was measured when self-excitation did not occur, as shown in Fig. 7 for a somewhat larger engagement, IL/R = 36.5% at LD = 0.0. A comparison with the unconstricted slip joint damping curves shows that the data sets were nearly similar at the same short IL/R and ζ_o, the exceptional data being those believed influenced by entrapped air. The similarity of the damping data sets is not surprising, since the unconstricted slip joint and one with an annulus constriction engaged at LD = 0.0 differ only in their entrance geometry. The similarity of the exit geometry of the two different slip joints supports the hypothesis of Section II that the flow emanating from the slip joints and impinging on the flexible tube is responsible for the self-excitation of essentially unconstricted slip joints.

As would be expected for similar damping data, the critical velocities for the square-edge constriction with LD = 0.0 and the slip joint with no constriction configuration are nearly the same. Compare the critical velocity data in the instability map of Fig. 11 with those in Fig. 4. Note that the ordinate in Fig. 11 is the ratio of the engaged constriction length (ICL) to the constriction gap ICL/W'. This allowed inclusion of data obtained for the configuration of Fig. 2(c) at several $0.7 \leq W'/R \leq 10.3\%$ with a nonzero LD/R = 18.3%. All the critical velocities for LD $\neq$ 0.0 were larger than those for LD = 0.0. Thus, the presence of an annulus upstream of a constriction must provide a source of positive damping, as discussed in Section II. Also, increasing the length of the constriction L for the same LD was observed to increase the critical velocity, as shown by the single data point in Fig. 11 for LD/R = L/R = 18.3%. This observation should not be unexpected, since increasing L for the unconstricted slip joint gave the same results.

The comparisons made above show that lower bounds on the flow damping and critical velocities for a square-edge annulus constriction at short engagement lengths, essentially an unconstricted slip joint, can be obtained from the data for a true unconstricted slip joint and all other parameters the same.

Thus the data of Figs. 4-8 are valuable for evaluation of a variety of slip joints, including one with a beveled annulus constriction.

Beveled Annulus Constrictions

Testing the beveled annulus constriction of Fig. 3(a) for BL < IL < BL + L gives a geometry that is hard to characterize. Always, a very short conical region will exist upstream of the constriction that, according to past discussions, should be a source of positive damping for the flow direction shown. For LD = 0.0, the flow emanating from the constriction will separate from the raised diameter and be farther away from the surface of the flexible tube than in the case of the unconstricted slip joint, Fig. 2(b). Since the impinging flow is believed to be the source of the self-excitation, critical velocities and damping should be larger for the beveled annulus constriction with all other parameters the same. For IL < BL + L, emanating flow will impinge immediately on part of the raised diameter of the constriction and then separate from the edge of the raised diameter, since L was not changed for these tests. Thus, the interaction with the flexible tube should be closer to the case of an unconstricted slip joint for smaller IL, but the mechanism still can be expected to be weaker because of the flow separation.

As expected, no self-excitation was observed for IL/R = 36.5% (LD = 0.0) and W'/R = 1.4%. Alone, the parallel flow through the long constriction length L = 1.0 in. (25.4 mm) provided enough positive damping to suppress self-excitation, based on unconstricted slip joint results. Actually, the damping for the beveled annulus constriction was slightly larger, as shown in Fig. 8, probably because of the presence of the conical upstream annulus (BL = 0.5 in. or 12.7 mm). For shorter engagements, IL/R = 18.3% and 9.1%, self-excitation was observed as shown in Fig. 11. The two data points suggest the critical velocities for the beveled annulus constriction at these short engagement lengths will approach those for the unconstricted slip joint. Of course, they will never be equal because of the positive damping provided by the conical upstream annulus. The damping values for the beveled annulus constriction also shown in Figs. 5 and 6 support this supposition.

V. CONCLUSIONS

Self-excitation mechanisms were observed to exist at short engagement lengths ($IL/R < 0.40$) for unconstricted slip joints and slip joints with short annulus constrictions ($L/W' \leq 12.5$), when the unsteady flow from the slip joint impinges on the flexible tube as shown in Figs. 3(b) and 2(c). For such short engagement lengths a slip joint with an annulus constriction essentially behaves as an unconstricted slip joint: the positive damping effect of any annulus between the tubes upstream of the annulus constriction is negligible. In fact, the mechanism existed when $IL < L$ for the sharp-edge annulus constriction of Fig. 2(c), or when $BL < IL < L + BL$ for the beveled annulus constriction of Fig. 3(a). Also, the critical velocity became smaller as IL was decreased. This trend was attributed to the known reduction in the positive, parallel flow damping that accompanies a reduction in the length or an increase in the width of the slip joint annular gaps. The source of the negative flow damping responsible for self-excitation is believed to be linked with the modulating pressure recovery forces acting on a flexible surface downstream from the vibrating slip joint, or any constriction subject to a constant pressure differential. A heuristic explanation of this self-excitation is given in Section II, where the mechanism for a center body flexibly mounted in a cylinder and subjected to annular flow with constrictions was expanded to include all the limiting cases of the slip joint for two telescoping tubes.

When the flow direction was reversed from that in Fig. 3(b), such that the unsteady flow into but not from the unconstricted slip joint impinged upon the flexible tube, the flow damping was observed to be positive for all unconstricted slip joints. Also, the flow damping increased with increased flowrate. In this case, positive damping is believed to be produced by the parallel flow in the gap between the tubes and by the unsteady flow converging along the wall of the flexible tube (A to C in Fig. 3(b)) before entering the modulating slip joint, as also explained in Section II. Also, positive damping was observed for slip joints with an upstream constriction and similar entry-flow conditions, but only at short engagement lengths. Positive damping does not prevail for slip joints with an annulus constriction at large engagement lengths ($LD >> L$) (Fig. 2(a)), because the annulus between the tubes downstream of the annulus constriction becomes an increasingly greater

source of negative damping as LD is increased. This annulus constriction self-excitation mechanism has been studied previously [1-9].

The unconstricted slip joint with the same engaged constriction length always had less flow damping and was more likely to be self-excited than the sharp-edge and beveled constrictions also tested (Figs. 2 and 3). Therefore, the results for an unconstricted slip joint can be used to bound the behavior of the other slip joints. Although critical velocities and flow damping were determined for large ranges of engagement lengths, gap sizes, and structural damping, understanding these details are not necessary for purposes of design. Self-excitation of essentially unconstricted slip joints occurs only for short engagement lengths and are easily avoided by maintaining engagement lengths greater than 20% of the diameter.

ACKNOWLEDGMENTS

This work was performed under the sponsorship of the Office of Basic Energy Sciences, U.S. Department of Energy.

REFERENCES

1. M. P. Paidoussis, "Flow-Induced Vibration in Nuclear Reactors and Heat Exchangers: Practical Experiences and State of Knowledge," in Practical Experiences with Flow-Induced Vibrations (E. Naudascher and D. Rockwell, eds.), Springer-Verlag, New York, pp. 1-81 (1980).

2. T. M. Mulcahy, "Leakage Flow-Induced Vibrations of Reactor Components," The Shock and Vibration Digest 15(9), 11-18 (1983).

3. M. W. Parkin, "Flow-Induced Vibration Problems in Gas Cooled Reactors," in Practical Experiences with Flow-Induced Vibrations (E. Naudascher and D. Rockwell, eds.), Springer-Verlag, New York, pp. 126-136 (1980).

4. T. M. Mulcahy, "Leakage Flow-Induced Vibration of a Tube-in-Tube Slip Joint," Symposium on Flow-Induced Vibration; Volume 4, Vibration Induced by Axial and Annular Flows (M. P. Paidoussis and M. K. Au-Yang, eds.), ASME, New York, pp. 15-24 (1984).

5. T. M. Mulcahy, "Avoiding Leakage Flow-Induced Vibration by a Tube-in-Tube Slip Joint," Argonne National Laboratory Report, ANL-84-82, Argonne, IL (1984). Also in Fluid-Structure Interaction and Aerodynamic Damping, ASME, New York, Sept. 1985, pp. 159-169.

6. T. M. Mulcahy, "Leakage Flow-Induced Vibration of an Eccentric Tube-in-Tube Slip Joint," Argonne National Laboratory Report, ANL-85-56, Argonne, IL (1985).

7. T. M. Mulcahy, "Leakage Flow-Induced Vibrations for Variations of a Tube-in-Tube Slip Joint," Argonne National Laboratory Report, ANL-86-11 (1986).

8. D. R. Miller, "Generation of Positive and Negative Damping with a Flow Restrictor in Axial Flow," Proceedings of the Conference on Flow-Induced Vibrations in Reactor System Components, Argonne National Laboratory Report, ANL-7685, pp. 304-307 (May 1970).

9. D. E. Hobson, "Fluid-Elastic Instabilities Caused by Flow in an Annulus," Presented at the 3rd Conference on Vibrations in Nuclear Plant, May 11-14, 1982, Keswick, English Lakes, U.K.

10. D. Mateescu and M. P. Paidoussis, "The Unsteady Potential Flow in an Axially Variable Annulus and Its Effects on the Oscillating Rigid Center-Body," Journal of Fluids Engineering 107, pp. 421-427 (1985).

11. T. Nakao, "Measurement of Leakage Flow Induced Vibrations of Cylinder," Journal of Nuclear Science and Technology 20(5), pp. 443-435 (1983).

12. S. S. Chen and M. W. Wambsganss, "Parallel-Flow-Induced Vibrations of Fuel Rods," Nuclear Engineering and Design 18, 253-278 (1972).

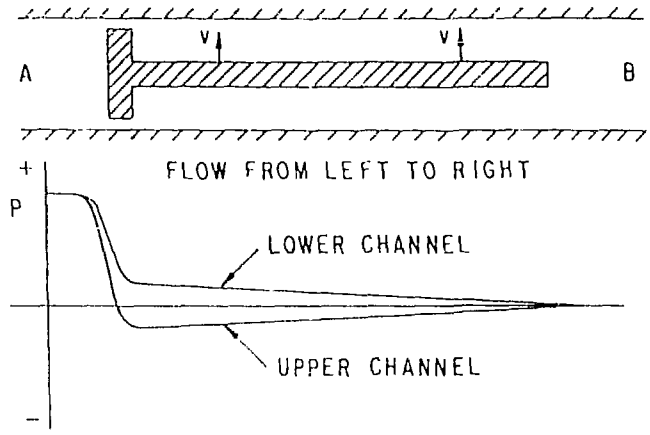

Fig. 1. Self-Excitation Mechanism Source

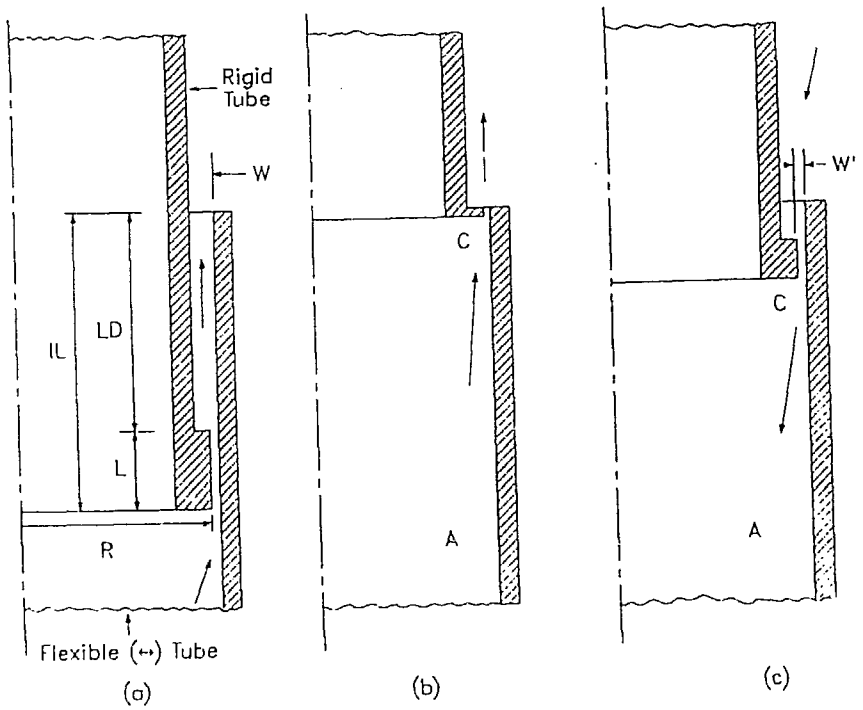

Fig. 2. Slip Joints with Sharp-Edge Annulus Constrictions: (a) Upstream Annulus Constriction, (b) No Downstream Annulus, (c) Downstream Annulus Constriction.

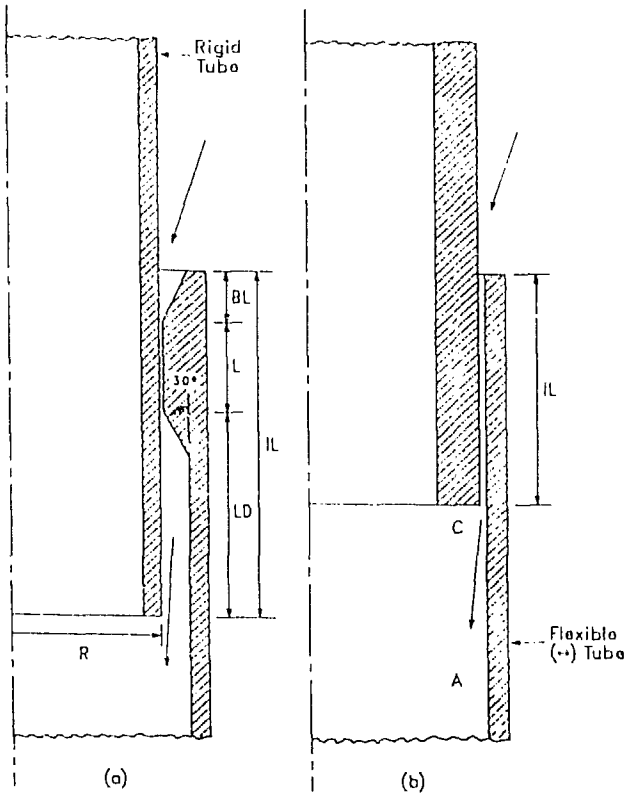

Fig. 3. Slip Joints with (a) An Upstream Beveled Annulus Constriction and (b) No Annulus Constriction.

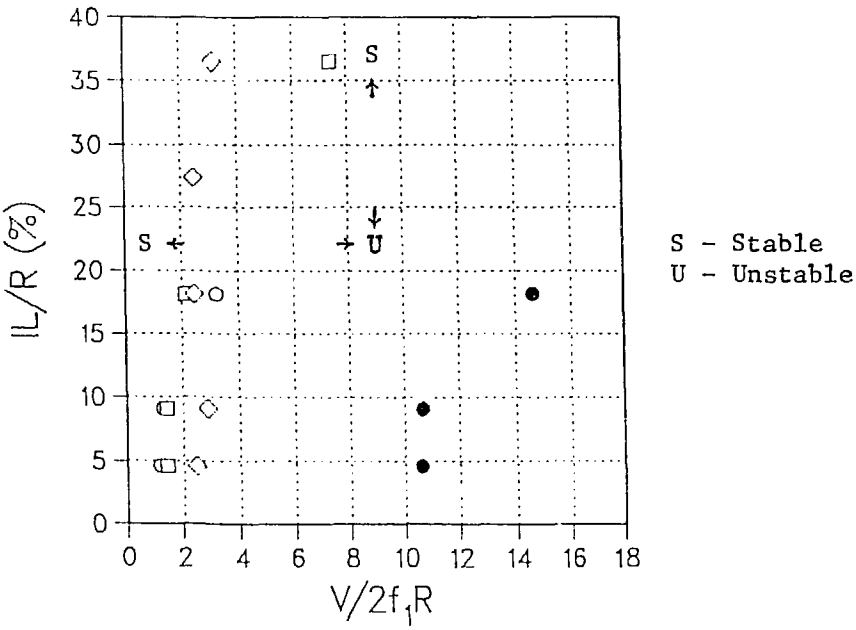

Fig. 4. Instability Map for Unconstricted Slip Joints with W'/R = 1.4%, ○ ; 5.2%, □ ; 10.3%, ◇. ζ_o ∿0.5% for open and ∿3% for solid symbols.

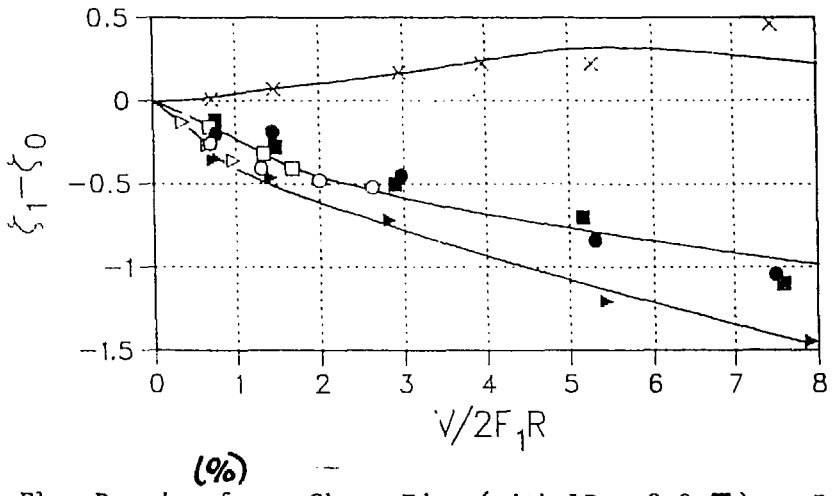

Fig. 5. Flow Damping, (%), for a Sharp-Edge (with LD = 0.0, □), a Beveled (×), and No (○) Annulus Constriction at W'/R = 1.4% and ICL/R = 18.3%. Also, an unconstricted slip joint is shown for IL/R = 4.6% (▷).

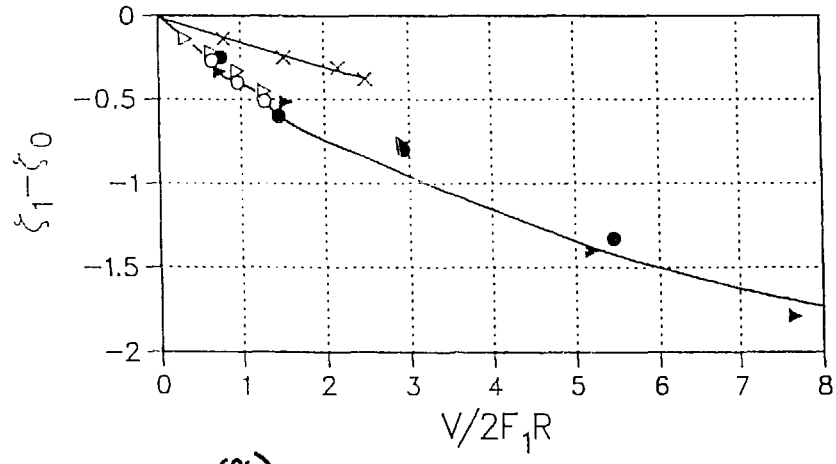

Fig. 6. Flow Damping, (%), for a Sharp-Edge (with LD = 0.0, ○), a Beveled (×), and No (◁) Annulus Constriction at W'/R = 1.4% and ICL/R = 9.1%.

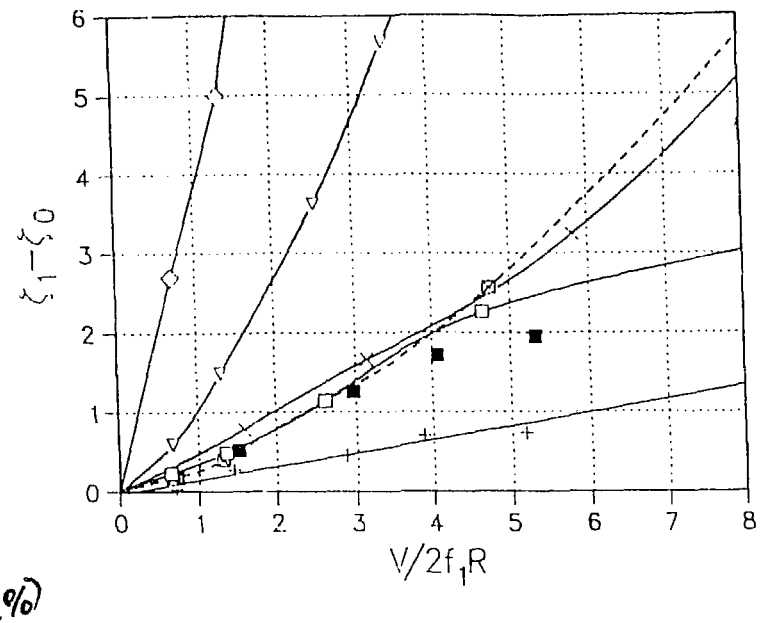

(%)

Fig. 7. Flow Damping at W'/R = 1.4% for an Unconstricted Slip Joint with IL/R (%) = 27.4, +; 36.5, □; 54.7, ▽; 109.5, ◇; 182.5, △. Also shown for ICL/R = 36.5% and LD = 0.0 is a square (⊠) and a beveled (×) Annulus Constriction.

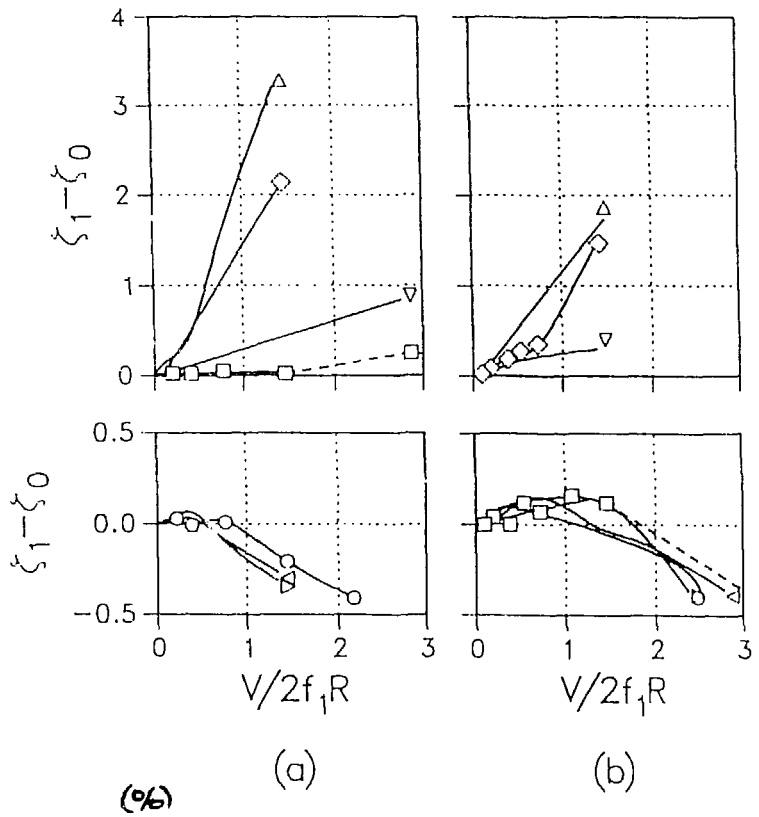

(%)

Fig. 8. Flow Damping for an Unconstricted Slip Joint at (a) W'/R = 5.2% and (b) W'/R = 10.3% with IL/R (%) = 4.6, ▷; 9.1, ◁; 18.3, ○; 36.5, □; 54.7, ▽; 109.5, ◇; 182.5, △.

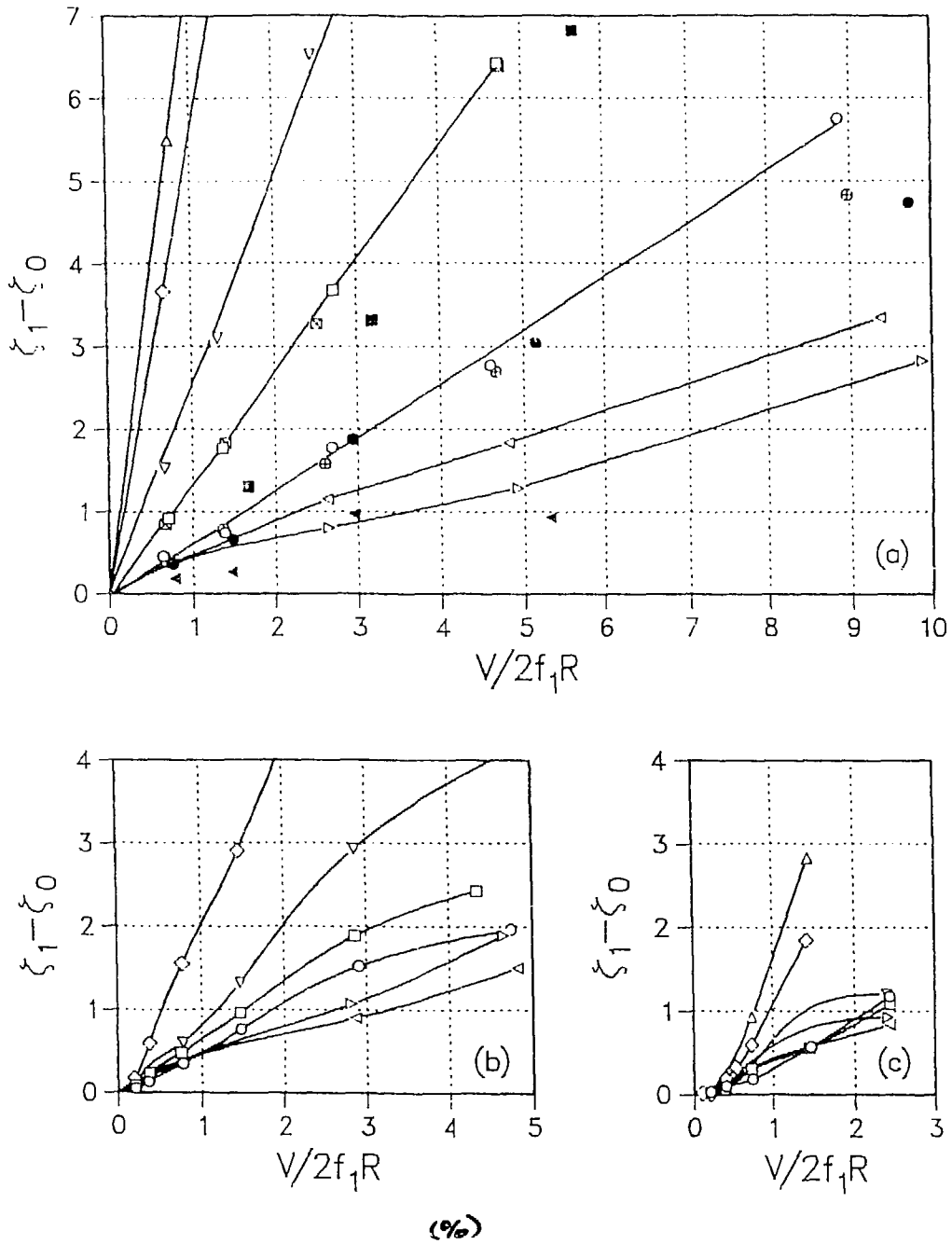

Fig. 9. Reversed Flow Damping for an Unconstricted Slip Joint with (a) W'/R = 1.4%, (b) W'/R = 5.1% and (c) W'/R = 10.3%, and ICL/R (%) = 182.5, △ ; 109.5, ◇ ; 54.8, ▽ ; 36.5, □ ; 18.3, ○ ; 9.1, ◁ ; and 4.6, ▷ . Also shown are sharp-edge (with LD = 0.0, ⊠ , ⊗) and beveled (■ , ● , ◀) annulus constrictions.

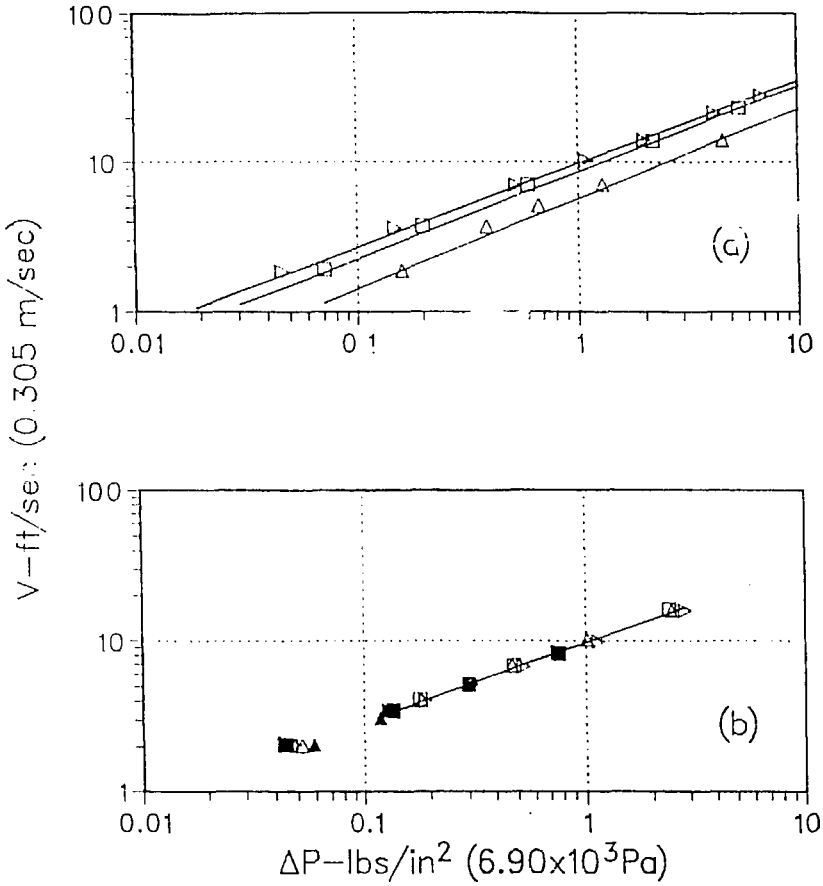

Fig. 10. Pressure Differentials for Unconstricted Slip Joints at W'/R = (a) 1.4%, (b) 5.1% and 10.3% (Solid Symbols) with IL/R (%) = 4.6, ▷ ; 36.5, □; 182.5, Δ .

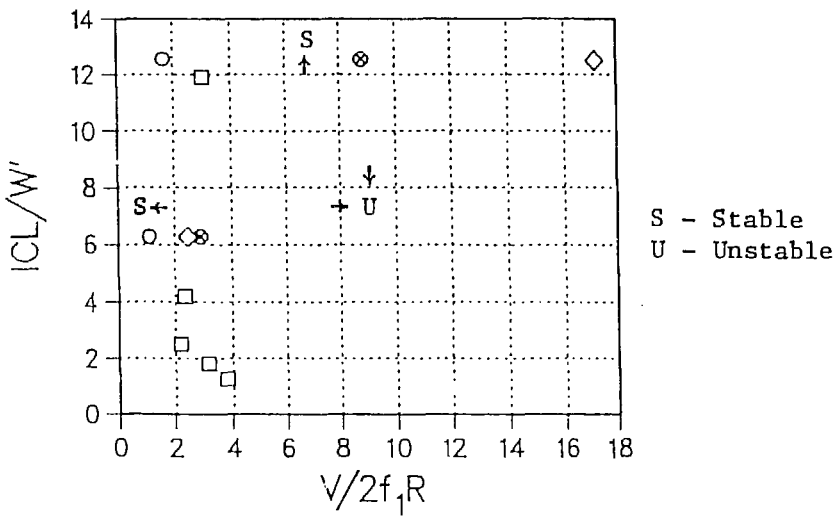

Fig. 11. Instability Map for a Sharp Edge Annulus Constriction with W'/R = 1.4% at LD/R = 0% (○) and 18.3% (◇), and with Variable W' (□) at L/R = 9.1% and LD/R = 18.3%. Also shown is a beveled annulus constriction with W'/R = 1.4% at LD/R = 18.3% (⊗).